Magnetic Properties of Co and Ni Multilayers on Diamond Surfaces

Bernd Stärk, Peter Krüger, and Johannes Pollmann

Institut für Festkörpertheorie, Westfälische Wilhelms-Universität Münster
48149 Münster, Germany
E-mail: {*bernd.staerk, kruger, pollman*}*@uni-muenster.de*

We present *ab initio* calculations of structural, electronic and magnetic properties of particular metal-semiconductor hybrid systems. They consist of Co multilayers on (111), as well as Co or Ni multilayers on (001) diamond surfaces. These systems are almost ideally lattice-matched. Our calculations for coverages of one up to six Co monolayers show that strong Co−C bonds are established across the interface giving rise to a large quenching of the magnetic moment at the Co interface layer. Yet, the spin polarisation at the Fermi level remains significantly large amounting to about $50\,\%$. This is a prerequisite for spintronic applications. In contrast, Ni adlayers on C(001) exhibit only a very small spin polarisation at the interface.

1 Introduction

Magnetism is a fascinating phenomenon that plays an important role in technological applications, as well as in basic research. The formation of magnetism in matter is a collective quantum mechanical effect. Generally speaking, the spins of the electrons align with respect to each other thus minimizing the total energy of the system. In case of parallel spin alignment the system becomes ferromagnetic.

Interestingly, magnetic properties of matter can strongly be influenced by reduced dimensions. Based on this fact, drastic improvements in information storage devices have been achieved recently by utilizing artificially structured magnetic materials[1–3]. Further substantial developments in computer technology seem to be accessible exploiting the fact that the carriers of electric currents have beside their charge also the spin as an additional degree of freedom. One example of so called spintronic devices is the spin field-effect transistor as proposed by Datta and Das[4]. This device uses the ability of ferromagnetic metals to generate spin-polarized currents which are transferred into the gate via ballistic transport. The role of the gate is to generate an effective magnetic field causing the spin to precess. By changing the voltage at the gate one can manipulate the orientation of the spins which can be detected at the ferromagnetic drain[3].

The gate is usually made of a semiconducting material. A thorough understanding of metal-semiconductor hybrid systems is of paramount importance, therefore. Of the multitude of conceivable hybrid systems[3,5–7] only very few are suitable for the aforementioned purposes. As has been shown previously, a useful hybrid system is required to have a good structural compatibility because a large lattice mismatch leads to diffusive transport processes[3]. These quickly destroy the magnetization of the currents induced by the source. A further prerequisite of a useful hybrid system is an energetic separation of the spin-up and spin-down states close to the Fermi level. Here, we discuss specific hybrid systems, namely Co and Ni adlayers on diamond surfaces, which are tailored to these particular needs and appear to be very promising, therefore.

Nowadays, there are powerful computational methods allowing for theoretical *ab initio* investigations[8] of such systems on high-performance computers. Using grants of computer time at the John von Neumann Institute for Computing (NIC) we have performed such studies of structural, electronic and magnetic properties of these systems.

After a brief overview of the employed computational methods in Section 2 we present some of our results for varying numbers of Co adlayers in Section 3. We conclude our discussion with a brief summary in Section 4.

2 Calculational Method

Our calculations are carried out in the framework of spin-density functional theory employing the generalized gradient approximation[9] for exchange and correlation. We use separable pseudopotentials[10,11] and include non-linear core-corrections[12] for a proper representation of structural and magnetic properties. Surfaces are simulated within the standard supercell approach using slabs containing six C substrate layers and up to six Co adlayers. Neighbouring supercells are decoupled by a vacuum region of at least 12 Å. Structure optimizations are carried out employing Hellmann-Feynman, as well as Pulay forces.

The wave functions are expanded in a basis set of atom-centred Gaussian orbitals of s, p, d and s^* symmetry. Since the d-component of the Co and Ni pseudopotentials is strongly localized, rapidly decaying Gaussian orbitals as well as a fine real-space mesh with up to one million points for an appropriate description of the investigated systems are used.

Integrations over the Brillouin zone are performed using special k-point sets[13]. To describe the spin polarization and magnetization properly a precise sampling of the Fermi surface is mandatory. Here, we use a $20 \times 20 \times 1$ **k**-point grid together with a Gaussian broadening of the density of states by 60 meV. For every **k**-point a generalized eigenvalue problem has to be solved which is the most time consuming part of the calculations. Since the diagonalizations for different **k**-points are independent of each other this step can however be massively parallelized.

Further very elaborate parts of our method are the calculation of the potential matrix elements and the charge density due to the fine real-space mesh. These evaluations are performed with very efficient algorithms, as suggested by Wieferink et al.[14]. For the charge density the procedure consists in first setting up the density matrix and subsequently evaluating the Gaussian basis functions on the mesh. In both steps the necessary calculations are independent for each pair of atoms. Building up the potential matrix elements also breaks up into independent calculations for atom pairs. In all cases a very high level of parallelization has been achieved leading to a very high overall scale-up of the program.

3 Results

3.1 Structural Properties

Cobalt is a ferromagnetic metal crystallizing in hcp and fcc structure depending on temperature and pressure. Under normal conditions the hcp structure is the standard modification. The fcc modification, on the other hand, can be stabilized by growing $Co_{0.92}Fe_{0.08}$ alloys[15]

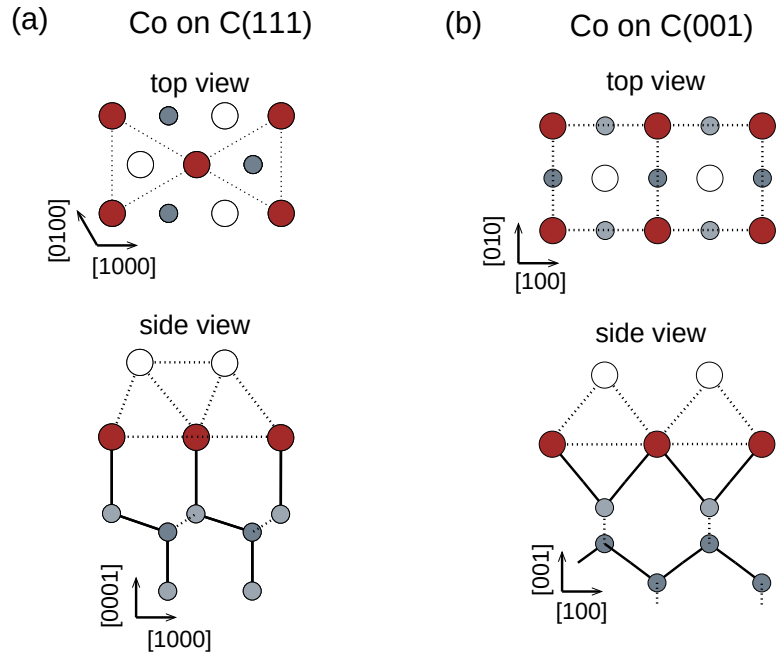

Figure 1. (a) Top and side view of one and two hcp Co adlayers on the C(111) surface. Large filled red circles mark Co atoms on the first and large open circles mark Co atoms on the second adlayer. Small blue circles indicate C substrate atoms. Full lines represent covalent sp^3 or pd bonds parallel to the drawing plane while dashed lines represent sp^3 bonds that form an angle with the drawing plane or metallic dd bonds. In the top view only dd bonds between Co atoms on the first adlayer are indicated by dashed lines. (b) Top and side view of one and two fcc Co adlayers on the C(001) surface.

and is furthermore the standard modification even at room temperature in Co nanoparticles[16].

The experimental lattice constants of Co are $a = 3.54\,\text{Å}$ for the fcc structure and $a = 2.51\,\text{Å}$ and $c = 4.07\,\text{Å}$ for the hcp structure. These lattice constants show an almost perfect matching with the surface lattice constants of $a_{\text{fcc}} = 3.57\,\text{Å}$ for C(001) and $a_{\text{hex}} = a_{\text{fcc}}/\sqrt{2} = 2.52\,\text{Å}$ for C(111). The lattice mismatch amounts to less than 1% in both cases. Therefore, the constituents of the metal-semiconductor hybrid system are highly compatible.

In the following, we discuss the structural properties of n Co layers adsorbed on a C(111) substrate surface, which will be referred to as n-Co:C(111). Starting with one Co adlayer, the energetically most favourable adsorption configuration is shown in Figure 1a. The Co adatoms are located above surface layer C atoms in *on top* positions. Thus, all substrate dangling bonds become saturated by the formation of one strong covalent Co−C bond per unit cell. This strong bond gives rise to a large binding energy of 1.9 eV per Co atom.

Since there is only a very small lattice mismatch between diamond and hcp cobalt, Co atoms of further adlayers adsorb in hcp bulk Co sites characteristic for a Co(0001) surface (large open circles in Figure 1(a)). The relaxed structures show some interesting trends in

the interlayer distances between neighbouring layers. First of all, the interlayer distances of the carbon layers show very little dependence on the number of Co adlayers. This implies a negligible impact of the Co layers on the structural properties of the substrate surface. In contrast, the Co layers in the slab show small contractions or expansions of their distances in an oscillatory manner, as compared to hcp bulk Co. This behaviour is in good agreement with the clean Co(0001) surface where similar oscillations occur. For thicker Co adlayers the interlayer distance in the middle of the adlayer converges toward the Co bulk interlayer distance, as one would expect. In total, we observe a fast and effective decoupling of all but the interface layer from the substrate.

The second kind of hybrid system investigated contains n layers of Co adsorbed on a C(001) substrate. For one Co adlayer the most stable adsorption site is a symmetric *bridge* site between neighbouring C surface atoms, as indicated in Figure 1b. In this case, the Co atoms reside in positions of an ideal diamond lattice on the first layer above the C(001) surface. They form two strong Co−C bonds which saturate all dangling bonds of the substrate surface. As a consequence, the binding energy of the Co adlayer is as large as 3.3 eV per unit cell.

Our structure optimization shows that Co atoms of further adlayers adsorb in fcc bulk Co sites (large open circles in Figure 1(b)). As in the case of Co on C(111), we observe an inward relaxation of the topmost Co adlayer together with an oscillatory behaviour of the interlayer spacings, as compared to the ideal fcc Co(001) surface. The general behaviour of the structural properties is very similar to that discussed above for Co adlayers on the C(111) surface.

A metal-diamond hybrid system with a small lattice mismatch can also be realized by replacing the Co atoms in the aforementioned structures by Ni atoms. Bulk Ni has a lattice constant a = 3.52 Å which is very close to that of fcc bulk Co. Our calculations show that the additional d electron per Ni atom has only a minor influence on the structural properties of nickel-diamond hybrid systems. The binding energy of a Ni adlayer is again very large with a value of 3.4 eV and the relaxations at the surface are comparable to those in the cobalt case.

3.2 Electronic and Magnetic Properties

The strong Co−C bonds at the interface, mentioned in the last section, have a large impact on the electronic structure for both systems. We start with a discussion of one Co adlayer on C(111). As noted above, the *on top* configuration of one Co monolayer on C(111) is characterized by the formation of one strong Co−C bond per unit cell. Figure 2 shows the spin-resolved band structures and densities of states (DOS) in the energy region near the Fermi level. We find seven bands in the projected band gap which result from the partially hybridized Co $4s$, Co $3d$ and C $2p$ states leading to a metallic surface. The spin-dependence of the bands is only very weak and does hardly change their dispersion. Based on a Mulliken analysis, we have marked the bands originating from both Co-$d_{3z^2-r^2}$ as well as C p_z states by thick lines in Figure 2. These orbitals give rise to the formation of an occupied bonding band B and a mostly unoccupied antibonding band B^*.

To further illustrate the character of these (anti-)bonding bands, Figure 3 shows charge density contours for the B and B^* states at the high-symmetry point K of the surface Brillouin zone. The bonding state B shows a large accumulation of charge density between

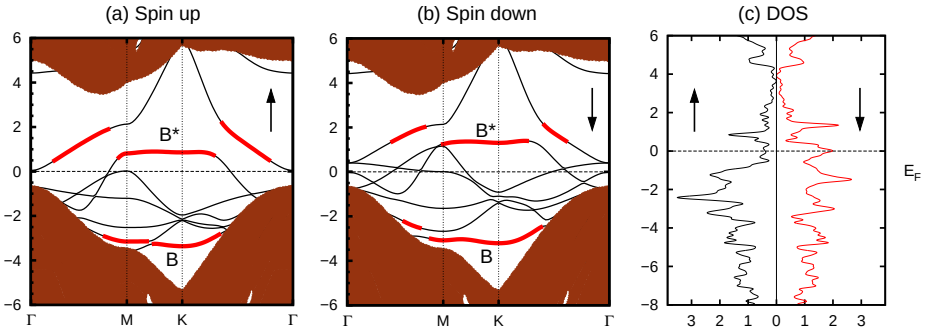

Figure 2. Band structures for (a) spin-up and (b) spin-down electrons and spin-resolved densities of states for one Co layer on the C(111) surface. The red shaded areas represent the projected band structure of bulk diamond. The band energies are referred to E_F as the zero energy.The band sections highlighted by thick lines originate from Co d states that have strong admixtures of C p states which are mainly localized at the atoms of the topmost C layer.

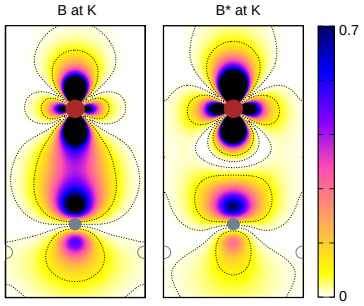

Figure 3. Charge density contours (in Å^{-3}) for the bonding (B) and antibonding (B*) state at the K point for the 1 Co:C (111) system. Large and small filled circles mark Co and C atoms, respectively, that are located in the drawing plane. The charge densities are plotted in the [1000]-[0001] plane containing the Co and C atom at the interface.

layer	1	2	3	4	5
μ_{Co6}					
μ_{Co5}					1.76
μ_{Co4}				1.78	1.60
μ_{Co3}			1.75	1.63	1.60
μ_{Co2}		1.76	1.51	1.56	1.53
μ_{Co1}	0.96	1.26	1.07	1.23	1.11
μ_{C1}	-0.09	-0.10	-0.13	-0.13	-0.13
μ_{C2}	0.02	0.03	0.03	0.03	0.03
ζ_{Co1}	-69	-51	-64	-50	-64
ζ_{C1}	-13	+6	+55	+31	+38
$\zeta^{\text{abs}}_{\text{Co1}}$	-1.56	-0.24	-1.09	-0.54	-0.84
$\zeta^{\text{abs}}_{\text{C1}}$	-0.01	-0.01	0.06	0.03	0.04

Table 1. Magnetic moment μ per atom and layer unit cell (in μ_B) and relative/absolute spin polarization $\zeta(E_F)$ per layer unit cell (in % resp. eV^{-1}) for n Co:C (111) hybrid systems.

the Co adlayer and C substrate top layer atom. In contrast, the charge density of the unoccupied state B^* has a nodal plane between the Co and C atom emphasizing its antibonding character.

Adding further Co adlayers to the system rapidly leads to an increase in the number of bands near the Fermi level so that the band structure becomes very congested. However, for all investigated hybrid systems with more than one adlayer they also turn out to be metallic. Furthermore we find the characteristic B and B^* bands near -3 and +1 eV originating from the Co−C interface bonds.

Layer-resolved magnetic moments are presented in Table 1 together with the respective

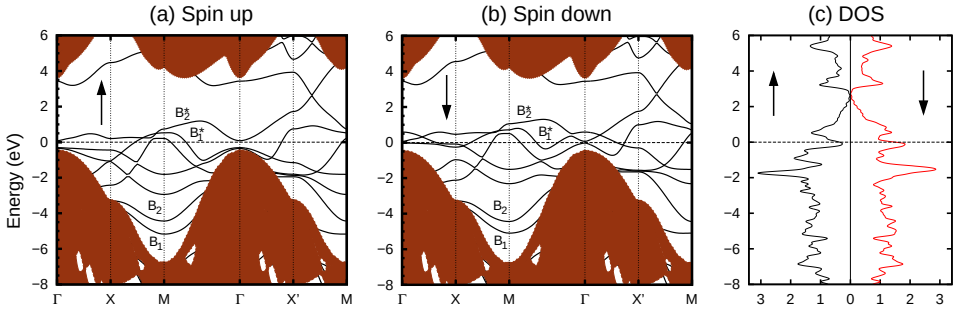

Figure 4. Band structures for (a) spin-up and (b) spin-down electrons and spin-resolved densities of states for one Co adlayer on the C(001) surface.

spin polarizations at E_F for varying numbers of adlayers. Some interesting features are to be noted. First of all, the formation of local magnetic moments is largely limited to the Co layers whereas the C layers remain essentially unmagnetized. Second, we observe that for each case the magnetic moment at the interface is considerably smaller than the respective value of a free-standing Co monolayer (μ=1.88 μ_B). This fact can be traced back to the formation of the B and B^* bands whose occupation is almost the same for both spin directions. As a result, the magnetic moment is drastically quenched at the interface, as compared to the free Co monolayer for which the occupation of the states in the flat region of the B^* band largely differs for the two spin directions. For more than one Co adlayer the local magnetic moments increase monotonously when going from the interface to the surface. At the topmost adlayer the magnetic moment per Co atom is close to that on a Co(0001) surface layer.

Another interesting quantity with regard to possible applications of these hybrid systems as part of a spintronic device is the relative spin polarization. It is defined via the spin resolved density of states as

$$\zeta(E) = \frac{N^{\uparrow}(E) - N^{\downarrow}(E)}{N^{\uparrow}(E) + N^{\downarrow}(E)} \tag{1}$$

and measures the surplus of spin-up states with respect to spin-down states at a certain energy. In Table 1 we show the relative spin polarisations at the Fermi energy for an increasing number of Co adlayers. A striking feature of the results is the substantial spin polarisation at the Co interface layer. The spin polarisation on the topmost C layer, on the other hand, is rather small and varies strongly for systems with different adlayer number.

For fcc cobalt layers on the C(001) surface the electronic structure becomes slightly more intricate since there are two Co$-$C bonds at the interface in this case. The band structure for one cobalt adlayer is presented in Figures 4a and 4b. The system is also metallic and the bands for spin-up and spin-down electrons are again rather similar. Yet the spin polarization at the Fermi level on the Co adlayer is about 50% also in this case. The interaction between the Co adlayer and the C(001) substrate now leads to two bonding (B_1 and B_2) and two antibonding (B_1^* and B_2^*) bands since there are two Co$-$C interface bonds per unit cell.

In Figure 5 we present associated charge densities at the $M-$point. The Co and C

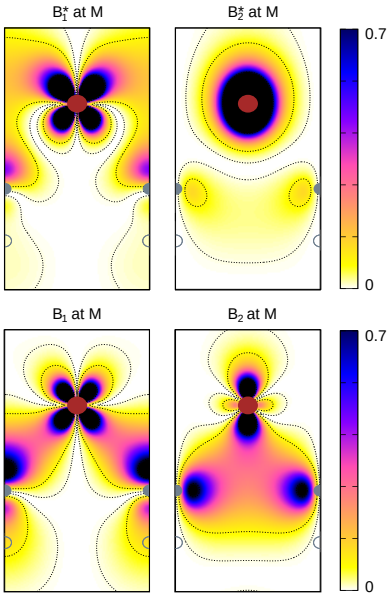

Figure 5. Charge densities at the M point of the surface Brillouin zone for the bonding (B_1 and B_2) and antibonding (B_1^* and B_2^*) states of one Co layer on C(001). The charge densities are plotted in the [100]-[001] plane containing the Co and the two C atoms at the interface.

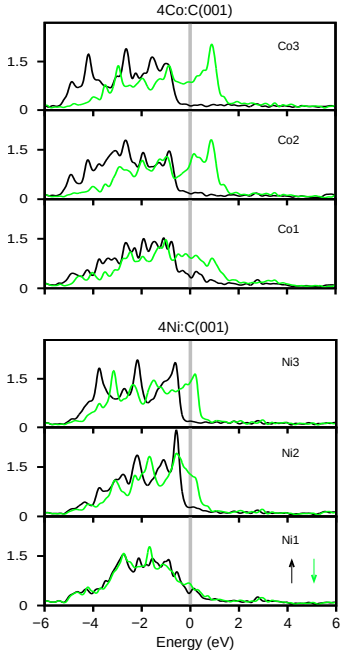

Figure 6. Layer-resolved densities of states for spin-up (black lines) and spin-down (green lines) electrons on the first three layers of systems containing four Co adlayers (upper panels) or four Ni adlayers (lower panels) on C(001), respectively.

orbitals form strong covalent bonds giving rise to considerably different spatial charge distributions for the B_1 and B_2 states. The double bonding leads to the large binding energy of 3.3 eV. The corresponding unoccupied antibonding states, on the other hand, exhibit a reduced screening in the spatial regions between the Co and C atoms.

Adding further layers of Co yields respectively more complex band structures. Here we only address layer-resolved densities of states (LDOS), therefore. As an example, we show in the upper three panels of Figure 6 the LDOS on the first three Co layers of a $4-\mathrm{Co{:}C}\,(001)$ system. One can immediately see that the spin-down LDOS on the second and third layer is shifted up by about 2 eV with respect to the spin-up LDOS near the Fermi level. This effect is strongly reduced for the first layer at the interface. On the first C layer at the interface, there is an appreciable LDOS within the gap energy region (not shown here), while on lower C layers the insulating behaviour of diamond is restored.

The two Co−C bonds per unit cell have significant consequences for the magnetic properties. The magnetic moment at the interface is only $0.42\mu_B$ and remains small for an increasing number of adlayers since the respective B_1, B_2 and B_1^*, B_2^* bands show almost no spin splitting. For more than one Co adlayer the magnetic moment of the top layer quickly converges to the value of the clean Co(001) surface.

The corresponding layer densities of states on the first three layers of a $4-\mathrm{Ni{:}C}\,(001)$

system are shown in the three lower panels of Figure 6. In general, the Co and Ni densities of states show a close resemblance. However, the spin splitting is drastically reduced for Ni as compared to the case of cobalt. This results from the additional d electron of each Ni atom occupying the spin-down states and shifting the respective LDOS to lower energies, therefore.

4 Concluding Remarks

In this article we have presented structural, electronic and magnetic properties of Co adlayers on C(111) and Co and Ni adlayers on C(001) as resulting from calculations in the framework of spin-density functional theory. The investigated systems are distinguished by an almost perfect matching of the lattice constants of their constituents. In all cases the strong covalent bonds established between adlayer and C substrate atoms give rise to a strong reduction of the local magnetic moment at the interface. Yet, for the systems with Co adlayers we find a high spin polarisation at the Fermi level even at the interface which is a prerequisite for spintronic applications. Ni adlayers, on the contrary, show only a very small spin polarisation at the interface.

Acknowledgements

We acknowledge financial support of this work by a grant of computer time on the JUMP computer of the John von Neumann Institute for Computing of the Forschungszentrum Jülich (Germany) under contract number HMS08-2961.

References

1. P. Grünberg, Rev. Mod. Phys. **80**, 1531 (2008).
2. A. Barthélémy, A. Fert, and F. Petroff, Handbook of Magnetic Materials, Vol. 12, edited by K. H. J. Buschow (Elsevier, Amsterdam, 1999).
3. I. Žutic, J. Fabian, and S. Das Sarma, Rev. Mod. Phys. **76**, 323 (2004).
4. S. Datta and B. Das, Appl. Phys. Lett. **56**, 665 (1990).
5. M. Hortamani, H. Wu, P. Kratzer, and M. Scheffler, Phys. Rev. B **74** , 205305 (2006).
6. L. Sacharow, M. Morgenstern, G. Bihlmayer, and S. Blügel, Phys. Rev. B **69**, 085317 (2004).
7. M. Zwierzycki, K. Xia, P. J. Kelly, G. E. W. Bauer, and I. Turek, Phys. Rev. B **67**, 092401 (2003).
8. R. Martin, *Electronic Structure*, (Cambride University Press, Cambridge, 2004).
9. J. P. Perdew, K. Burke and M. Ernzerhof, Phys. Rev. Lett. **77**, 3865 (1996).
10. L. Kleinman, and D. M. Bylander, Phys. Rev. Lett. **48**, 1425 (1982).
11. D. R. Hamann, Phys. Rev. B **40**, 2980 (1989).
12. S. G. Louie, S. Froyen, and M. L. Cohen, Phys. Rev. B **26**, 1738 (1982).
13. H. J. Monkhorst and J. D. Pack, Phys. Rev. B **13**, 5188 (1976).
14. J. Wieferink, P. Krüger and J. Pollmann, Phys. B **74**, 205311 (2006).
15. S. M. Shapiro and S. C. Moss, Phys. Rev. B **15**, 2726 (1977).
16. R. N. Grass and W. J. Stark, J. Mater. Chem. **16**, 1825 (2006).